Reanalysis of the decay $K_L \to \pi^0 e^+ e^-$

John F. Donoghue and Fabrizio Gabbiani
Department of Physics and Astronomy, University of Massachusetts, Amherst, Massachusetts 01003
(Received 1 September 1994)

The decay $K_L \to \pi^0 e^+ e^-$ is searched for as a signal of direct $\Delta S = 1$ CP violation. We provide a thorough updating of the analysis of the three components of the decay: (1) direct CP violation, (2) CP violation through the mass matrix, and (3) CP-conserving (two photon) contributions. First the chiral calculation of the $K_S \to \pi^0 e^+ e^-$ rate, due to Ecker, Pich, and de Rafael, is updated to include recent results on the nonleptonic amplitude. Then we systematically explore the uncertainties in this method. These appear to be so large that they will obscure direct CP violation unless it is possible to measure the $K_S \to \pi^0 e^+ e^-$ rate. The CP-conserving amplitude remains somewhat uncertain, but present indications are such that there may be a sizable CP-violating symmetry in the e^+, e^- energies from the interference of the CP-conserving and CP-violating amplitudes and this may potentially be useful in determining whether direct CP violation is present.

PACS number(s): 13.20.Eb, 11.30.Er, 12.15.Ji, 12.39.Fe

I. INTRODUCTION

One of the goals of the next generation of rare kaon decay experiments is to attempt to observe CP violation in the decay $K_L \to \pi^0 e^+ e^-$. This reaction is special because we expect that direct CP violation (as opposed to the "mass matrix" CP violation already observed in the parameter ϵ) may be the dominant component of the amplitude. This is in contrast with $K_L \to \pi\pi$, where the direct effect is, at most, a few parts in a thousand of ϵ. Direct CP violation distinguishes the standard model from "superweak"-type models [1]. Moreover, the magnitude of the direct CP violation for this reaction is a precise prediction of the standard model, with very little hadronic uncertainty. In this article, we will update the analysis of the reaction $K_L \to \pi^0 e^+ e^-$, attempting to understand if we can be certain that an experimental measurement is in fact a signal of direct CP violation.

One difficulty is that there are three possible components to the decay amplitude: (1) a CP-conserving process which proceeds through two photon exchanges, (2) a mass-matrix CP-violating effect proportional to the known parameter ϵ, and (3) the direct $\Delta S = 1$ CP violating effect which we would like to observe. The existence of the first of these indicates that simply observing the total decay rate is not sufficient to indicate unambiguously the existence of CP violation. We need to either observe a truly CP-odd decay asymmetry, or else be confident on the basis of a theoretical calculation that the CP-conserving effect is safely smaller than the experimental signal. Unfortunately, the predictions in the literature for each of the components listed above exhibit a range of values, including some estimates where all three are similar in magnitude. However, the quality of the theoretical treatment can improve with time, effort, and further experimental input. We will try to assess the present and future uncertainties in the theoretical analysis.

There remain significant experimental difficulties before it is possible to mount a search sensitive to a branching ratio of a few times 10^{-12}. We will assume that such a sensitivity is reached. At the same time, it is reasonable to assume that we will have improved experimental information on the related rate $K_L \to \pi^0\gamma\gamma$, and that theoretical methods will have provided a consistent phenomenology of this reaction. The Kobayashi-Maskawa (KM) parameters will be somewhat more fully constrained in the future, but hadronic matrix element uncertainties will prevent a precise determination of the parameters relevant for CP violation, at least until B meson CP violation has been extensively explored. With these expectations as our framework, will we be able to prove that the future experimental observation indicates the presence of direct CP violation?

Our analysis indicates that one will not be able to prove the existence of direct CP violation from the branching ratio for $K_L \to \pi^0 e^+ e^-$ unless the decay rate for the related decay $K_S \to \pi^0 e^+ e^-$ is also observed experimentally. This is yet more difficult than measuring the K_L decay, and poses a problem for the program of finding direct CP violation. It is possible but not certain that the electron charge asymmetry can resolve this issue and, when combined with the rate, signal direct CP violation.

II. OVERVIEW OF THE ANALYSIS

There is an extensive analysis associated with each of the three components of the decay amplitude which were listed in the Introduction. We will devote separate sections of the paper to each of the major issues. The purpose of the present section is to highlight the main issues which are to be discussed more fully later, and to indicate how they fit together in an overall description of the decay process.

In a way, the direct CP component is the simplest. The uncertainties are only in the basic parameters of the standard model, i.e., the mass of the top quark and the

KM parameters. The relevant hadronic matrix element is reliably known. Unfortunately the extraction of KM elements has significant uncertainties, so that only a range of possible values can be given. This range corresponds to $K_L \to \pi^0 e^+ e^-$ branching ratios of a few times 10^{-12}. We discuss this range in Sec. III.

The contribution of mass-matrix CP violation is more uncertain. The rate due to this source is given by the parameter ϵ times the rate for $K_S \to \pi^0 e^+ e^-$, so that the issue is the prediction of the CP-conserving K_S partial rate. Here the primary tool is chiral perturbation theory, with the pioneering treatment given by Ecker, Pich, and de Rafael (EPR) [2,3]. In Sec. IV, we update their analysis, under essentially the same assumptions. The main new ingredient is the inclusion of the results of the one-loop analysis of nonleptonic decays, which decreases the overall strength of the weak $K \to \pi$ transition. This yields a change in the weak counterterms and a decrease of the rate. However, more important is an assessment of the uncertainties of such a calculation, which we describe in Sec. V. Any such calculation has a range of uncertainties, most of which we are able to estimate based on past experience with chiral calculations. We systematically discuss these. Unfortunately we find that one issue in particular has a devastating sensitivity on this mode. In their analysis, EPR made an assumption which lies outside of chiral perturbation theory, that a certain weak counterterm satisfies $w_2 = 4L_9$ where L_9 is a known coefficient in the QCD-effective chiral Lagrangian. This assumption has no rigor, and the decay rate is very sensitive to the deviation $w_2 - 4L_9$. For any reasonable value of direct CP violation, there is an equally reasonable value of w_2 which can reproduce the corresponding $K_L \to \pi^0 e^+ e^-$ decay rate. Given a measurement, we will then be intrinsically unable to decide if it is evidence of a nonzero value of direct CP violation or merely measures a value for w_2. It is this which indicates a need to measure the rate $K_S \to \pi^0 e^+ e^-$.

The third component is the CP-conserving amplitude which proceeds through the two photon intermediate state $K_L \to \pi^0 \gamma\gamma, \gamma\gamma \to e^+ e^-$, described in Sec. VI. Here we must first understand the process $K_L \to \pi^0 \gamma\gamma$. This has been calculated in chiral perturbation theory at one-loop order and has been measured experimentally. While the shape agrees with the chiral calculation, the theoretical rate misses by a factor of 3. This has prompted some reanalyses of the theory of $K_L \to \pi^0 \gamma\gamma$, which we will take account of. However, the field has not reached a full conclusion on this mode, and it is clear that in the future the experimental and phenomenological status of this reaction will undoubtedly improve. We study how possible resolutions of these analyses will influence the $K_L \to \pi^0 \gamma\gamma$ decay rate. Ultimately this component should be satisfactorily understood.

The ultimate problem is then our inability to distinguish, in a measurement of the $K_L \to \pi^0 e^+ e^-$ decay rate, the direct CP violation from the mass-matrix effect. It is possible that the electron energy asymmetry may allow us to make this separation. The electron asymmetry comes from the interference of the CP-conserving two photon process (even under the interchange of $e^+ e^-$) and the CP-violating one photon process (odd under the $e^+ e^-$ interchange). For many values of the presently favored parameter range, this asymmetry is very large, i.e., of order 50%. In this case its measurement is not far more difficult than a good measurement of the rate. If we, in fact, are able to reach an understanding of the two photon process, through future phenomenology and experiments on $K_L \to \pi^0 \gamma\gamma$, then the asymmetry depends most critically on the CP-violating amplitude. If there is no direct CP violation, there is then a correlation between the $K_L \to \pi^0 e^+ e^-$ decay rate and the electron asymmetry, parametrized by the unknown coefficient w_2. As we detail in Sec. VII, the presence of direct CP violation would upset this correlation, and in many cases would lead to a drastically different relative size of the asymmetry vs decay rate, often even changing the sign of the asymmetry. Thus the asymmetry may be used to signal direct CP violation. Unfortunately this method is not foolproof. There exist combinations of values of w_2 and KM angles for which the distinction between direct and mass-matrix CP violation are not so great and will be muddied by the inherent uncertainties in the theory. In Sec. VIII we explore the use of K_L-K_S interference to sort out the direct CP-violating amplitude.

Overall, our reanalysis indicates that the demands on the experimental exploration of this reaction are quite severe. The simple observation of a few events will not be sufficient to indicate direct CP violation. The measurement of an electron asymmetry requires more events, and may or may not resolve the issue. Only the simultaneous measurement of $K_S \to \pi^0 e^+ e^-$ allows a convincing proof of the existence of direct CP violation.

III. DIRECT CP VIOLATION

Direct $\Delta S = 1$ CP violation is manifested in the "penguin" reaction pictured in Fig. 1. The QCD short-distance corrections to this mode have been thoroughly analyzed to next-to-leading order by Buras *et al.* [4], and we will use their results. The primary weak operators responsible for the transition have the form

$$\mathcal{H}_W = \frac{G_F}{\sqrt{2}}[C_{7V}(\mu) Q_{7V} + C_{7A} Q_{7A}], \tag{1}$$

where

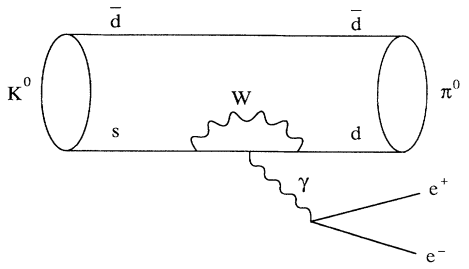

FIG. 1. "Penguin" diagram inducing $\Delta S = 1$ CP violation.

$$Q_{7V} = (\bar{s}d)_{V-A}(\bar{e}e)_V,$$
$$Q_{7A} = (\bar{s}d)_{V-A}(\bar{e}e)_A. \quad (2)$$

The dominant contribution to the imaginary part of the coefficient C_{7i} comes from the top quark, so that this is truly a short distance process. The coefficients have a CP-violating component

$$\mathrm{Im}C_{7i} = -\mathrm{Im}\left(\frac{V_{td}V_{ts}^*}{V_{ud}V_{us}^*}\right) y_{7i}, \quad (3)$$

with the results of Ref. [4] yielding

$$\frac{y_{7V}}{\alpha} = \begin{cases} 0.708 & m_t = 150, \\ 0.743 & m_t = 175, \\ 0.775 & m_t = 200, \end{cases} \quad \frac{y_{7A}}{\alpha} = \begin{cases} -0.579 & m_t = 150, \\ -0.736 & m_t = 175, \\ -0.905 & m_t = 200, \end{cases} \quad (4)$$

with very little dependence on $\Lambda_{\overline{\mathrm{MS}}}$ (the above is for $\Lambda_{\overline{\mathrm{MS}}} = 0.3$ GeV, where $\overline{\mathrm{MS}}$ denotes the modified minimal subtraction scheme) and a negligible dependence on the low energy scale μ.

The matrix element involved is well known via isospin symmetry from the charged current kaon decay, i.e.,

$$\langle \pi^0(p')|\bar{d}\gamma_\mu s|K^0(p)\rangle = \frac{f_+(q^2)}{\sqrt{2}}(p+p)_\mu + \frac{f_-(q^2)}{\sqrt{2}}(p-p')_\mu, \quad (5)$$

with

$$f_+(q^2) = 1 + \lambda q^2, \qquad \lambda = (0.65 \pm 0.005)\ \mathrm{fm}^2. \quad (6)$$

The form factor f_- does not contribute significantly to the decay because its effect is proportional to m_e. The decay rate is

$$B(K_L \to \pi^0 e^+ e^-)_{\mathrm{dir}} = 4.16(\mathrm{Im}\lambda_t)^2(y_{7A}^2 + y_{7V}^2),$$

$$\mathrm{Im}\lambda_t = \mathrm{Im}V_{td}V_{ts}^* = |V_{ub}||V_{cb}|\sin\delta = A^2\lambda^5\eta, \quad (7)$$

where $V_{td} = |V_{ub}|\sin\delta$, and A, λ, η, referred to the Wolfenstein parametrization of the KM matrix [5]. This results in

$$B(K_L \to \pi^0 e^+ e^-)_{\mathrm{dir}} = \left\{ \begin{array}{l} 2.1 \times 10^{-12} \\ 2.75 \times 10^{-12} \\ 3.6 \times 10^{-12} \end{array} \right\} \times \left(\frac{\mathrm{Im}\lambda_t}{10^{-4}}\right)^2 \quad \text{for } m_t = \begin{cases} 150\ \mathrm{GeV} \\ 175\ \mathrm{GeV} \\ 200\ \mathrm{GeV} \end{cases}. \quad (8)$$

The dependence on the top quark mass will of course be removed by a convincing precise measurement of m_t.

The KM parameter V_{cb} has the most favored values (including the recent CLEO data) [6]

$$V_{cb} = \begin{cases} 0.036 \pm 0.002 \pm 0.002 & \text{heavy quark effective theory (HQET)}, \\ 0.036 \pm 0.002 \pm 0.003 & B \to D^* l\nu \text{ models}, \\ 0.039 \pm 0.001 \pm 0.004 & B \to X l\nu, \\ 0.036 \pm 0.003 & \text{(averaged)}. \end{cases} \quad (9)$$

The element V_{ub} is measured by the inclusive decay $B \to X_u e\nu$ in the electron endpoint region. The two inclusive calculations available yield

$$\frac{V_{ub}}{V_{cb}} = \begin{cases} 0.082 \pm 0.006 & \text{[Altarelli, Cabibbo, Corbo, Maiani, and Martinelli (ACCMM)] [7]}, \\ 0.074 \pm 0.007 & \text{[Ramirez, Donoghue, and Burdman (RDB)] [8]}. \end{cases} \quad (10)$$

Models that calculate a set of exclusive decays ($B \to Me\nu$) can only be used to provide an upper bound on V_{ub} since there are many final states (such as $B \to \pi\pi e\nu$ with $\pi\pi$ nonresonant) that are not calculated. These limits are

$$\frac{V_{ub}}{V_{cb}} \le \begin{cases} 0.12 & \text{[Isgur, Stora, Grinstein, and Wise (ISGW)] [9]}, \\ 0.087 & \text{[Wirbel, Stech, and Bauer (WSB)] [10]}, \\ 0.067 & \text{[Körner and Schuler (KS)] [11]}. \end{cases} \quad (11)$$

We will use the former measurements to estimate

$$\left|\frac{V_{ub}}{V_{cb}}\right| = 0.078 \pm 0.007 \pm 0.010, \quad (12)$$

with the first uncertainty experimental and the second theoretical. In the Wolfenstein parametrization of the KM matrix, the values of V_{cb} and V_{ub} imply

$$A = 0.74 \pm 0.06,$$
$$\sqrt{\rho^2 + \eta^2} = 0.355 \pm 0.056. \quad (13)$$

Without any further analysis, these measurements imply an upper bound on $\mathrm{Im}\lambda_t$:

$$\begin{aligned}\mathrm{Im}\lambda_t &= |V_{ub}||V_{cb}|\sin\delta \\ &= (1.0 \pm 0.3) \times 10^{-4}\sin\delta. \end{aligned} \tag{14}$$

A lower bound on this parameter can be found by consideration of the analysis of ϵ. In the Wolfenstein parametrization one has the approximate form [4]

$$|\epsilon| = (3.4 \times 10^{-3}) A^2 \eta B_K \left[1 + 1.3A^2(1-\rho)\left(\frac{m_t}{m_W}\right)^{1.6}\right], \tag{15}$$

where B_K parametrizes the hadronic matrix element and is estimated to be in the range $0.33 \leq B_K \leq 1$. Using $(1-\rho) < 1.4$ and $B_K < 1$ one finds

$$A^2\eta \geq \begin{cases} 0.104, & m_t = 200 \text{ GeV}, \\ 0.13, & m_t = 175 \text{ GeV}, \\ 0.16, & m_t = 150 \text{ GeV}, \end{cases} \tag{16}$$

so that

$$\mathrm{Im}\lambda_t = A^2\lambda^5\eta \geq \begin{cases} 5.3 \times 10^{-5}, & m_t = 200 \text{ GeV}, \\ 6.8 \times 10^{-5}, & m_t = 175 \text{ GeV}, \\ 8.2 \times 10^{-5}, & m_t = 150 \text{ GeV}. \end{cases} \tag{17}$$

This brackets the range

$$0.53 \times 10^{-4} \leq \mathrm{Im}\lambda_t \leq 1.3 \times 10^{-4}. \tag{18}$$

Note that $\mathrm{Im}\lambda_t$ is positive. These constraints yield a decay rate from direct CP violation of magnitude

$$\left.\begin{matrix}1.01\\1.25\\1.4\end{matrix}\right\} \times 10^{-12} \leq B(K_L \to \pi^0 e^+ e^-)_{\mathrm{dir}} \leq \left\{\begin{matrix}6.1\\4.6\\3.5\end{matrix}\right\} \times 10^{-12} \text{ for } m_t = \left\{\begin{matrix}200\\175\\150\end{matrix}\right. . \tag{19}$$

Alternatively, the "best" values

$$\begin{aligned}\mathrm{Im}\lambda_t &= 1.0 \times 10^{-4}, \\ m_t &= 175 \text{ GeV}, \end{aligned} \tag{20}$$

which we will take as our standard reference values, lead to a rate

$$B(K_L \to \pi^0 e^+ e^-)_{\mathrm{dir}} = 2.32 \times 10^{-12}. \tag{21}$$

A more detailed analysis including a correlation between ρ and η inherent in Eq. (15), as well as the use of $B_d^0\bar{B}_d^0$ mixing (which constrains $A\sqrt{(\rho-1)^2+\eta^2}$ as a function of f_B) narrows the range only slightly because hadronic uncertainties dominate.

IV. REVISING THE EPR ANALYSIS

In this section, we review the formalism for analyzing mass-matrix CP violation, first set forth by Ecker, Pich, de Rafael (EPR) [2,3]. This amounts to the prediction of the decay rate for $K_S \to \pi^0 e^+ e^-$, since the mass-matrix effect is defined by

$$\begin{aligned} A(K_L \to \pi^0 e^+ e^-)|_{\mathrm{MM}} &\equiv \epsilon A(K_S \to \pi^0 e^+ e^-), \\ \epsilon &= (2.258 \times 10^{-3}) e^{i\pi/4}. \end{aligned} \tag{22}$$

We then redo the results taking into account recent work on the nonleptonic kaon decays to one-loop order. While this produces a significant numerical change, it is more important as a prelude to our subsequent analysis of uncertainties in the analysis.

The prediction of $K_S \to \pi^0 e^+ e^-$ comes from a comparison with $K^+ \to \pi^+ e^+ e^-$, which contains many of the same ingredients. The reactions are displayed schematically in Figs. 2 and 3. In these diagrams the round circles represent the electromagnetic coupling, while the square boxes indicate the action of the weak interaction. We know the electromagnetic interactions of pions and kaons from direct measurement. The weak $K \to \pi$ transition of Fig. 2(a) and (b) is known within some theoretical uncertainty from the use of chiral symmetry to relate it to $K \to 2\pi$ and $K \to 3\pi$. However the weak $K\pi\gamma$ vertex is not known *a priori* and needs to be extracted from the analysis of $K^+ \to \pi^+ e^+ e^-$.

The nonleptonic weak interactions are described by effective chiral Lagrangians, organized in an expansion in powers of the energy, or equivalently in numbers of derivatives and masses. At lowest order, called order E^2, the physical transitions are described by a unique Lagrangian

$$\begin{aligned} \mathcal{L} &= G_8 \mathrm{Tr}(\lambda_6 D_\mu U D^\mu U^\dagger), \\ U &\equiv \exp\left(i\frac{\lambda^A \cdot \phi^A}{F_\pi}\right), \quad A = 1, \ldots, 8, \end{aligned} \tag{23}$$

where ϕ^A are the octet of pseudoscalar mesons (π, K, η). At next order, order E^4, the number of possible forms of Lagrangians is quite large, and has been categorized by Kambor, Missimer, and Wyler [12]. Not all of these contribute to $K \to 2\pi$ and $K \to \pi$, but certain linear combinations do influence these amplitudes. The formalism of chiral perturbation theory dictates that when an analysis is carried out to order E^2, that one use Eq. (23) at the tree level, in which case one obtains from the $K \to \pi$

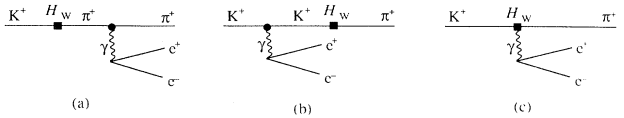

FIG. 2. Diagrams contributing to the reaction $K^+ \to \pi^+ e^+ e^-$. Round circles represent the electromagnetic coupling while the square boxes indicate the action of the weak interaction.

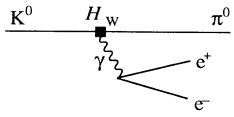

FIG. 3. Same as in Fig. 2 for $K_L \to \pi^0 e^+ e^-$.

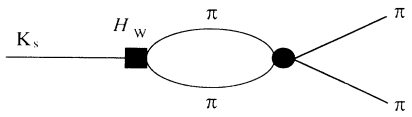

FIG. 4. One-loop diagrams involving $\pi\pi$ rescattering in the $I = 0$ channel for $K_S \to (\pi\pi)_{I=0} \to (\pi\pi)_{I=0}$. The notation for vertices is as in Fig. 2.

decay rate

$$G_8 = \frac{G_F}{\sqrt{2}} |V_{ud} V_{us}^*| g_8,$$
$$g_8^{\text{tree}} = 5.1. \tag{24}$$

Note that we neglect the CP violation in the nonleptonic amplitude, contained in G_8, because this is bounded to be tiny by the smallness of ϵ'/ϵ.

In contrast, when evaluated at order E^4, one must include one-loop diagrams in addition to the possible order E^4 Lagrangian. The loop diagrams involving $\pi\pi$ rescattering in the $I = 0$ channel, $K \to (\pi\pi)_{I=0} \to (\pi\pi)_{I=0}$ as pictured in Fig. 4, are quite large and are the major part of the order E^4 analysis. While there is some ambiguity in the extraction of g_8 (see below), the enhancement from $\pi\pi$ rescattering leads to a smaller value of g_8, with a good estimate being [13]

$$g_8^{\text{loop}} = 4.3. \tag{25}$$

The $K \to \pi$ amplitude used in Figs. 2 and 3 does not have the enhancement from $\pi\pi$ rescattering, and is given in terms of g_8 by

$$A(K^+ \to \pi^+) = 2 G_8 k^2,$$
$$A(K^0 \to \pi^0) = -\sqrt{2} G_8 k^2. \tag{26}$$

We will explore further uncertainties in the $K \to \pi$ vertex in the next section.

To complete the diagrams of Figs. 2 and 3 requires the electromagnetic vertices of kaons and pions. In chiral perturbation theory to order E^4 these are given by

$$\langle \pi^+ | J^\mu | \pi^+ \rangle = \left\{ 1 + q^2 \left[\frac{2 L_9(\mu)}{F_\pi^2} - \frac{1}{96\pi^2 F_\pi^2} \left(\ln \frac{m_\pi^2}{\mu^2} + \frac{1}{2} \ln \frac{m_K^2}{\mu^2} + \frac{3}{2} \right) \right] \right\} (p + p')^\mu,$$
$$\langle K^+ | J^\mu | K^+ \rangle = \left\{ 1 + q^2 \left[\frac{2 L_9(\mu)}{F_\pi^2} - \frac{1}{96\pi^2 F_\pi^2} \left(\ln \frac{m_K^2}{\mu^2} + \frac{1}{2} \ln \frac{m_\pi^2}{\mu^2} + \frac{3}{2} \right) \right] \right\} (p + p')^\mu. \tag{27}$$

The first of these is known more fully from experiment, and has the form

$$\langle \pi^+ | J^\mu | \pi^+ \rangle = \frac{(p + p')^\mu}{[1 - q^2/m^2]},$$
$$m = 730 \text{ MeV}. \tag{28}$$

Taylor expanding the latter form one determines $L_9(\mu = m_\eta) = (7.4 \pm 0.7) \times 10^{-3}$. The experimental charge radii,

$$\langle r^2 \rangle_{\pi^+} = (0.44 \pm 0.02) \text{ fm}^2,$$
$$\langle r^2 \rangle_{K^+} = (0.34 \pm 0.05) \text{ fm}^2, \tag{29}$$

are compatible with this value. The final ingredient required for Figs. 2(c) and 3 is the weak photonic coupling. This includes both short distance and long distance physics, as illustrated in Fig. 5. While the short distance components have a reliable hadronic matrix element (it is due to the real parts of the coefficients discussed in the previous section), the QCD coefficient depends strongly on the low energy cutoff μ. In the full matrix element, this dependence is canceled by a corresponding dependence on μ of the long distance physics. However since the long distance physics is not calculable, we must attempt to determine this coupling phenomenologically. The innovation of EPR was to elucidate the possible forms that this coupling could take. They found that there were two possible chiral Lagrangians which could contribute to this process:

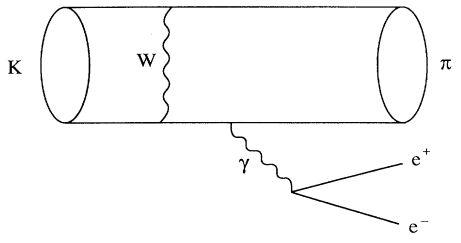

FIG. 5. Diagrams contributing to the short distance weak photonic coupling for $K \to \pi e^+ e^-$.

$$\mathcal{L}_W = \frac{ieG_8}{2} F^{\mu\nu}[w_1 \mathrm{Tr}(Q\lambda_{6-i7}\mathcal{L}_\mu\mathcal{L}_\nu) + w_2 \mathrm{Tr}(Q\mathcal{L}_\mu\lambda_{6-i7}\mathcal{L}_\nu)],$$
$$\mathcal{L}_\mu \equiv -(\partial_\mu U - ie[A_\mu, U])U^\dagger = -(D_\mu U)U^\dagger. \quad (30)$$

In the presence of the short distance electroweak penguin effect due to Z exchange with an axial electron coupling, we need a third effective Lagrangian, not present in EPR:

$$\mathcal{L}'_W = \frac{i2\pi\alpha}{3} G_8 w_5 \bar{e}\gamma^\mu\gamma_5 e\, \mathrm{Tr}(\lambda_{6-i7}\mathcal{L}_\mu). \quad (31)$$

The correspondence with the notation of the last section is

$$\mathrm{Im}w_5 = \frac{3}{4\pi}\frac{1}{|V_{ud}V_{us}^*|g_8}\frac{y_{7A}}{\alpha}\mathrm{Im}\lambda_t. \quad (32)$$

Note that the labeling of w_5 takes into account the Lagrangians labeled by w_3, w_4 defined by EPR [2,3,14] which contributed to other radiative K decays. In fact this form of $\mathcal{L}'_W$ is closely related to the w_1 term since by using identities of the U matrix it can be shown that

$$\begin{aligned} F^{\mu\nu}\mathrm{Tr}(Q\lambda_{6-i7}\mathcal{L}_\mu\mathcal{L}_\nu) &= -F^{\mu\nu}\partial_\nu \mathrm{Tr}(Q\lambda_{6-i7}\mathcal{L}_\nu) \\ &= (\partial_\mu F^{\mu\nu})\mathrm{Tr}(Q\lambda_{6-i7}\mathcal{L}_\nu), \\ &= (-e)\bar{e}\gamma_\mu e\mathrm{Tr}(Q\lambda_{6-i7}\mathcal{L}_\nu), \\ &= \left(\frac{e}{3}\right)\bar{e}\gamma_\mu e\mathrm{Tr}(\lambda_{6-i7}\mathcal{L}_\nu), \end{aligned} \quad (33)$$

where in the second line we have integrated by parts, thus we subsequently used the equation of motion so that

$$\frac{ieG_8}{2}F_{\mu\nu}w_1\mathrm{Tr}(Q\lambda_{6-i7}\mathcal{L}_\mu\mathcal{L}_\nu) = \frac{i\pi\alpha G_8}{3}w_1\bar{e}\gamma_\mu e\mathrm{Tr}(\lambda_{6-i7}\mathcal{L}_\nu). \quad (34)$$

This allows us to identify the short distance CP-violating part of w_1:

$$\mathrm{Im}w_1 = \frac{3}{4\pi}\frac{1}{|V_{ud}V_{us}^*|g_8}\frac{y_{7V}}{\alpha}\mathrm{Im}\lambda_t. \quad (35)$$

The real parts of w_1, w_2 contain long distance contributions and hence are not predictable by present techniques. They need to be extracted from experimental measurements. The other process available for this procedure is $K^+ \to \pi^+e^+e^-$ (unless $K_S \to \pi^0e^+e^-$ is measured in the future). Unfortunately one cannot fix both w_1, w_2 in this way, so that one must add a theoretical assumption in order to proceed. The relevant amplitudes are

$$\begin{aligned} \mathcal{M}(K^+ \to \pi^+e^+e^-) &= \frac{G_8\alpha}{4\pi}d_+(p+p')^\mu\bar{u}\gamma_\mu v, \\ \mathcal{M}(K_S \to \pi^0e^+e^-) &= -\frac{G_8\alpha}{4\pi}d_S(p+p')^\mu\bar{u}\gamma_\mu v, \\ \mathcal{M}(K_L \to \pi^0e^+e^-) &= -\frac{G_8\alpha}{4\pi}(p+p')^\mu\bar{u}[d_V\gamma_\mu + d_A\gamma_\mu\gamma_5]v, \end{aligned} \quad (36)$$

with

$$\begin{aligned} d_+ &\equiv w_+ + \phi_K(q^2) + \phi_\pi(q^2), \\ d_S &\equiv \mathrm{Re}w_S + 2\phi_K(q^2), \\ w_+ &= -\frac{16\pi^2}{3}(w_1^r + 2w_2^r - 12L_9^r) - \frac{1}{6}\ln\frac{m_K^2m_\pi^2}{m_\eta^4}, \\ w_S &= w_+ + 16\pi^2(w_2^r - 4L_9^r) + \frac{1}{6}\ln\frac{m_\pi^2}{m_K^2}, \\ \phi_i(q^2) &= \frac{m_i^2}{q^2}\int_0^1 dx\left[1 - \frac{q^2}{m_i^2}x(1-x)\right] \\ &\quad \times\ln\left[1 - \frac{q^2}{m_i^2}x(1-x)\right], \end{aligned} \quad (37)$$

and for the CP-violating K_L decay

$$\begin{aligned} d_V &= \epsilon d_S - \frac{16\pi^2}{3}i\mathrm{Im}w_1, \\ d_A &= \frac{16\pi^2}{3}i\mathrm{Im}w_5. \end{aligned} \quad (38)$$

The goal of the search for direct CP violation is to separate the $\mathrm{Im}w_{1,5}$ terms from the mass-matrix effect ϵd_S. Note that in these expressions we have neglected the possible direct CP violation in the $K \to \pi$ transition (which is bounded to be very small by the measurement of ϵ'/ϵ) and the contribution of $\mathrm{Re}w_5$ to CP-conserving decays (since $\mathrm{Re}w_5 \approx \mathrm{Im}w_5 \ll \mathrm{Re}w_1$).

The EPR analysis of $K^+ \to \pi^+e^+e^-$ uses the tree level value of $g_8, g_8^{\mathrm{tree}} = 5.1$. The decay rate is consistent with two values of $\mathrm{Re}w_+$, and a subsequent analysis of the decay spectrum favored the lower value for $\mathrm{Re}w_+$, i.e., $\mathrm{Re}w_+ = 1.16 \pm 0.08$ [2]. However, given that one is working to one-loop order, it is more consistent to use the one-loop value for $g_8, g_8^{\mathrm{loop}} = 4.3$. Because of the presence of the L_9 term, this is not just a rescaling of the value of w_+. An additional change that we make is to use the known full electromagnetic vertex in the pole diagrams, rather than just the first term in the expansion of the form factor. Note that because of the factor of $k \cdot p$ in the weak matrix element, the only significant form factor is that of the pion in Fig. 2. This implies the replacement

$$\frac{2L_9^r}{F_\pi^2} \to \frac{2L_9^r}{F_\pi^2(1 - q^2/m_\rho^2)} \quad (39)$$

in the formula for w_+. The associated logarithms with $\mu \approx m_\eta$ are much smaller than the L_9^r dependence and are not influenced much by this replacement. As a technical note, we comment that some potential modifications using a phenomenological pion form factor could lead to a lack of gauge invariance. By modifying the coefficient of a gauge-invariant effective Lagrangian, we preserve the gauge-invariant nature of the amplitude. With these changes, we find

$$\mathrm{Re}w_+ = 1.01 \pm 0.10 \quad (40)$$

[without the second change, we would have had $\mathrm{Re}w_+ = 1.33 \pm 0.065$]. This is illustrated in Fig. 6.

One cannot simply transfer this information to K_S or

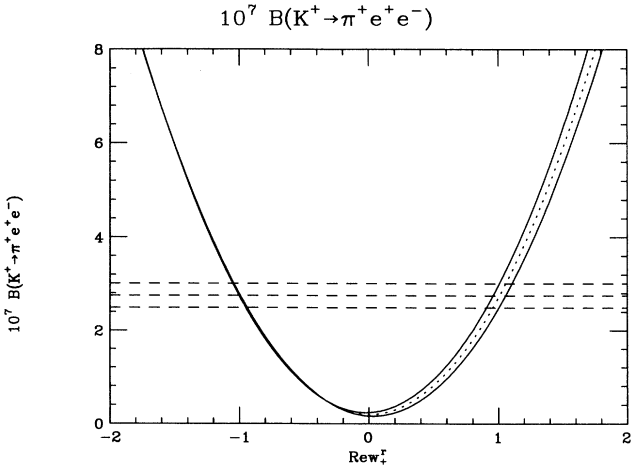

FIG. 6. The branching ratio $B(K^+ \to \pi^+ e^+ e^-)$ is plotted against Rew_+. The solid curves are obtained using the extreme values of the error intervals of $|V_{ud}| = 0.9753 \pm 0.0006$, $|V_{us}| = 0.221 \pm 0.003$, and $L_9(m_\eta) = (7.4 \pm 0.7) \times 10^{-3}$, while the dashed curve corresponds to the central values. The experimental value of the branching ratio $\pm$ its experimental errors are indicated by dashed horizontal lines.

K_L decays, because a different linear combination enters

$$w_S = w_+ + 16\pi^2(w_2 - 4L_9) + \frac{1}{6}\ln\frac{m_\pi^2}{m_K^2}. \tag{41}$$

However EPR deal with this problem by making the assumption that $w_2 = 4L_9$ resulting in Re$w_S = 0.73 \pm 0.08$ [2]. They note that this is an assumption which is not part of chiral perturbation theory, but do not explore the consequences if it is not correct. We will discuss this in the next section, finding a very strong sensitivity. At this stage we note that if one makes the assumption of $w_2 = 4L_9$, one obtains Re$w_S = 0.58 \pm 0.10$ for our value of Rew_+.

At this value of w_S, the direct and mass-matrix contributions are comparable:

$$\begin{aligned} d_V &= \epsilon d_S - \frac{16\pi^2}{3} i\mathrm{Im}w_1 \\ &\approx e^{i\pi/4}(0.57 \times 10^{-3}) - i1.0 \times 10^{-3}, \\ d_A &= i1.0 \times 10^{-3}, \end{aligned} \tag{42}$$

when evaluated with $m_t = 175$ GeV, Im$\lambda_t = 10^{-4}$. This leads to a branching ratio

$$B(K_L \to \pi^0 e^+ e^-)_{\mathrm{MM}} = 0.37 \times 10^{-12} \tag{43}$$

if there is no direct CP violation (Im$\lambda_t = 0$) (EPR found $B_{\mathrm{MM}} = 1.5 \times 10^{-12}$ in this case [3]), vs

$$B(K_L \to \pi^0 e^+ e^-)_{CP} = 1.78 \times 10^{-12} \tag{44}$$

for the full set of parameters given above in Eq. (37). The addition of mass-matrix CP violation in this analysis led to a small decrease in the rate compared to the purely direct CP violation of the previous section, Eq. (21), because of the cancellation in the imaginary part of d_V. However this may change if $w_2 \neq 4L_9$.

One of the results that we will see in the next section is that the mass-matrix contribution to the branching ratio is near a minimum value when w_2 is close to $4L_9$. For other values of w_2, the rate can easily be an order of magnitude larger. Although our value for the branching ratio is a factor of four below that of EPR, both estimates are similar in saying that the mass-matrix contribution will be small as long as $w_2 = 4L_9$.

Using the tree level value for $g_8, g_8^{\mathrm{tree}} = 5.1$, the mass-matrix contribution to the branching ratio is

$$B(K_L \to \pi^0 e^+ e^-)_{\mathrm{MM}} = 0.55 \times 10^{-12}. \tag{45}$$

V. UNCERTAINTIES IN MASS-MATRIX CP VIOLATION

Our goal in this section is to assess how well we understand the prediction for $K_S \to \pi^0 e^+ e^-$. The most important effect will be discussed in subsection C below, but we proceed systematically to discuss even contributions which have less uncertainty.

A. Purely electromagnetic vertices

The electromagnetic vertices enter in diagrams 2, 3(a) and (b). The uncertainty here is in the choice of whether to use the chiral expansion of the form factor truncated at order q^2, Eq. (27), or the full q^2 dependence of the monopole form factor, Eqs. (28) and (39). The first choice is natural when one is working to a given order in the chiral energy expansion, but the latter choice clearly includes more of the physics which is known about the electromagnetic vertex. Note that it is essentially only the pion's form factor which is relevant, because the diagram involving the kaon's form factor, Fig. 2(b), is suppressed by a factor of m_π^2/m_K^2 with respect to Fig. 2(a) because of the momentum dependence of the weak $K \to \pi$ transition. The use of the full form factor produces a modest variation in the value of w_+ (i.e., Re$w_+ = 1.01$ instead of Re$w_+ = 1.33$). Because of cancellations in the K^0 amplitude this provokes a more extreme variation on the decay rate. The lowest-order chiral vertex, Eq. (27), produces a decay rate

$$B(K_L \to \pi^0 e^+ e^-)_{\mathrm{MM}} = 1.96 \times 10^{-12} \tag{46}$$

instead of the result of Eq. (43). [We note that if we had also modified w_2 in the same way as $4L_9$ as in Eq. (39) we would have a $B(K_L \to \pi^0 e^+ e^-)_{\mathrm{MM}} = 1.33 \times 10^{-12}$.] While we feel that it is good physics to use the full electromagnetic form factor, one could also interpret these results as an uncertainty in the analysis due to higher-order terms in q^2, with that uncertainty being of order 2×10^{-12}.

B. The weak $K \to \pi$ vertex

We have already given one indication of the sensitivity of the result to the size of the $K \to \pi$ transition. Under otherwise identical assumptions, $g_8^{\rm tree} = 5.1$ yielded the rate in Eq. (45), while $g_8^{\rm loop} = 4.3$ produced the result of Eq. (43). These modifications to g_8 also include corresponding modifications to the $K\pi\gamma$ vertex required by gauge invariance. This is automatically maintained, however, by the use of gauge-invariant effective Lagrangians. In order to appreciate that this change in g_8 is not the only uncertainty in the $K\pi$ amplitude, one needs to understand a bit more about the chiral phenomenology of $K \to 2\pi$ and $K \to 3\pi$.

Chiral symmetry relates processes with different numbers of pions, such as $K \to \pi$ vs $K \to 3\pi$. The predictions are compactly contained in the chiral Lagrangians, but can also be obtained using the soft pion theorems, which was the methodology used in the 1960's. The only advantage of the latter technique is that it relies only on chiral SU(2) while modern chiral Lagrangian analysis have always involved chiral SU(3) symmetry. [Presumably the latter could be reformulated in chiral SU(2), but no one has yet done this.] The soft pion analysis indicates that one obtains the same relation (up to terms of order m_π^2) between $K \to 2\pi$ and $K \to 3\pi$ for any Lagrangian which survives in any soft pion limit of $K \to 3\pi$ (i.e., $p_i \to 0$). The only Lagrangians which do not survive in any soft pion limit involve four separate derivatives on the four fields of $K \to 3\pi$, e.g.,

$$\mathcal{L}_{\rm quartic} = \frac{g_8}{\Lambda_1^2}{\rm Tr}(\lambda_6 D_\mu U D_\nu U^\dagger D^\mu U D^\nu U^\dagger). \tag{47}$$

This Lagrangian yields a matrix element proportional to $(k \cdot p_1)(p_2 \cdot p_3)$ which clearly vanishes as any $p_i \to 0$. In contrast most of the order E^4 Lagrangians do not vanish in all soft pion limits. An example is

$$\mathcal{L}' = \frac{g_8}{\Lambda_2^2}{\rm Tr}(U^\dagger \lambda_6 D_\mu D_\nu U D^\mu U^\dagger D^\nu U), \tag{48}$$

which then yields the same relations of $K \to 3\pi$ and $K \to 2\pi$ as does the lowest-order result $\mathcal{L}$ given in Eq. (23). (This phenomenon is explained in more detail in Ref. [15].) Since the only inputs to the chiral phenomenology are the amplitudes for $K \to 2\pi$ and $K \to 3\pi$, it follows that one cannot distinguish a combination $\mathcal{L} + \mathcal{L}'$ from a Lagrangian involving $\mathcal{L}$ only.

However, when we discuss the $K \to \pi$ vertex, there *is* a distinction between these various Lagrangians. For example $\mathcal{L}'$ in Eq. (48) involves a minimum of three meson fields, and hence contributes to $K \to 2\pi$ and $K \to 3\pi$ but not at all to $K \to \pi$. In contrast, the lowest-order Lagrangian Eq. (23) contributes to all of $K \to \pi$, $K \to 2\pi$, $K \to 3\pi$. Since known phenomenology cannot distinguish between linear combinations of $\mathcal{L} + \mathcal{L}'$, this manifests itself in an uncertainty in the $K \to \pi$ vertex. Since the higher-order Lagrangians are known to make a 25% difference in relation between $K \to 2\pi$ and $K \to 3\pi$, it would be unreasonable to take this uncertainty in $K \to \pi$ to be any less than 25–30%. Using $g_8 = 4.3 \times (1 \pm 30\%)$ yields a range

$$B(K_L \to \pi^0 e^+ e^-)_{\rm MM} \sim 10^{-16} - 1.5 \times 10^{-12}. \tag{49}$$

This again indicates that the analysis has significant cancellations present and that modest variations in the analysis can lead to uncertainties of order 1.5×10^{-12}.

C. The $K\pi\gamma$ vertex

The parameter w_+ was determined from the analysis of $K^+ \to \pi^+ e^+ e^-$. This arrangement has some intrinsic uncertainty because it was performed to a given order in the chiral energy expansion. It would be reasonable to take this uncertainty at 30%.

However, this uncertainty is dwarfed by the errors introduced by the assumption of $w_2 = 4L_9$. There is nothing about chiral symmetry which forces such a relation. For example, if the process of Fig. 7 were to contribute to the weak coupling, the relation $w_2 = 4L_9$ would not occur except for a special value of the $K \to a_1, f_1$ amplitude. This is highly unlikely, and we can easily accept $w_2 - 4L_9 \neq 0$. The crucial distinction here is between models and rigorous theory. Chiral perturbation theory is a rigorous method which expresses true relationships in QCD to a given order in the energy expansion. However, an assumption such as $w_2 = 4L_9$ may be true or false in a way that we cannot decide based on QCD. It may occur within some models, yet we have no guidance as to whether it is correct in nature. We cannot base something as important as the observation of the direct CP violation on something as flimsy as a model.

Unfortunately the decay rate for $K_S \to \pi^0 e^+ e^-$ depends very strongly on the value of w_2. This strong dependence was observed by Littenberg and Valencia [16]. If we were to chose $w_2 = 0$, the rate would be two orders of magnitude larger. In Fig. 8 we plot the branching ratio for the mass-matrix contribution to $K_L \to \pi^0 e^+ e^-$ vs w_2. We see that for reasonable values of w_2, we get a wide range of values of the branching ratio. Conversely, a measured value of $B(K_L \to \pi^0 e^+ e^-)$ in the range of $10^{-12} \to$ few $\times 10^{-11}$ could be interpreted in terms of a reasonable value of w_2. This is then an enormous uncertainty in the mass-matrix contributions to $K_L \to \pi^0 e^+ e^-$. This uncertainty could be removed if one measured the rate of $K_S \to \pi^0 e^+ e^-$. The mass matrix contribution would then be known, see Eq. (22). However, this task is not easy experimentally.

VI. THE CP-CONSERVING AMPLITUDE

The $K_L \to \pi^0 e^+ e^-$ transition can also take place through a CP-conserving two photon intermediate state. If we ignore the electron mass, the form of the amplitude

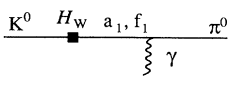

FIG. 7. Diagram contributing to the weak photon coupling. The notation for the vertices is as in Fig. 2.

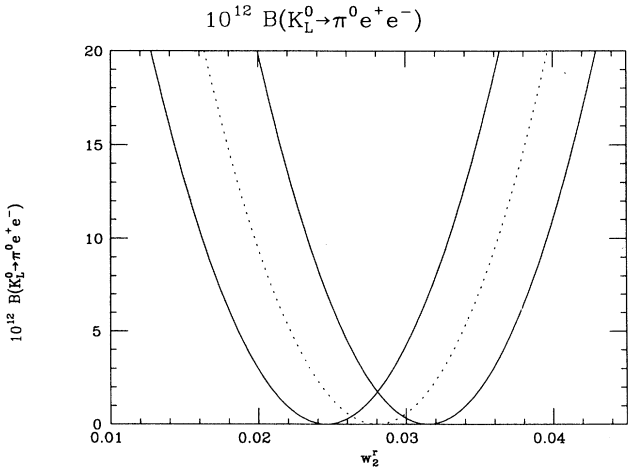

FIG. 8. The mass matrix contribution for the branching ratio $B(K_L \to \pi^0 e^+ e^-)_{\rm MM}$ is plotted against w_2. The convention for the solid and dashed curves is the same as for Fig. 6.

will be

$$\mathcal{M}(K_L \to \pi^0 e^+ e^-)_{\rm CPC}$$

$$= G_8 \alpha^2 K p \cdot (k_{e^+} - k_{e^-})(p + p')^\mu \bar{u} \gamma_\mu v, \tag{50}$$

where K is a form factor and the extra antisymmetry under $k_{e^+} \leftrightarrow k_{e^-}$ is a reflection of the properties under a CP transformation. In order to calculate this, we need to understand the $K_L \to \pi^0 \gamma\gamma$ transition first.

We are fortunate that $K_L \to \pi^0 \gamma\gamma$ is accessible to present experiments, and significant phenomenology has been performed on this reaction. We will utilize the work of Cohen, Ecker, and Pich [17] as representative of present work, with the understanding that future experimental and theoretical work will clarify the analysis considerably. The $K_L \to \pi^0 \gamma\gamma$ amplitude has two form factors A, B, defined via

$$\mathcal{M}(K_L \to \pi^0 \gamma\gamma) = \frac{G_8 \alpha}{4\pi} \epsilon_\mu(q_1) \epsilon_\nu(q_2) \Big[A(q_2^\mu q_1^\nu - q_1 \cdot q_2 g^{\mu\nu}) + 2\frac{B}{m_K^2}(k \cdot q_1 q_2^\mu p^\nu + p \cdot q_2 q_1^\nu p^\mu - q_1 \cdot q_2 p^\mu p^\nu - g^{\mu\nu} p \cdot q_1 p \cdot q_2) \Big]. \tag{51}$$

When the photons couple to e^+e^-, as in Fig. 9, it is well known that the A amplitude contributes to $K_L \to \pi^0 e^+ e^-$ only proportional to m_e, which is a small effect which we will drop. It is the B amplitude which is important for the e^+e^- final state. The authors use a representation which fits the known $K_L \to \pi^+\pi^-\pi^0$ amplitude in a dispersive treatment of $K_L \to \pi^0\gamma\gamma$ and find

$$\begin{aligned}
B(x) &= c_2 \left\{ \frac{1}{x} F(x) + \frac{4}{3}(5 - 2x) \left[\frac{1}{6} + R(x) \right] + \frac{2}{3} \ln \frac{m_\pi^2}{m_\rho^2} \right\} + \beta - 8 a_V, \\
x &= \frac{(k_{e^-} + k_{e^+})^2}{4 m_\pi^2}, \\
\beta &= -0.13, \\
c_2 &= 1.11, \\
F(x) &= 1 - \frac{1}{x} [\arcsin(\sqrt{x})]^2, \quad x \le 1, \\
&= 1 + \frac{1}{4x} \left[\ln \frac{1 - \sqrt{1 - 1/x}}{1 + \sqrt{1 - 1/x}} + i\pi \right]^2, \quad x \ge 1, \\
R(x) &= -\frac{1}{6} + \frac{1}{2x} \left[1 - \sqrt{1/x - 1} \arcsin(\sqrt{x}) \right], \quad x \le 1, \\
&\quad -\frac{1}{6} + \frac{1}{2x} \left[1 + \sqrt{1 - 1/x} \left(\ln \frac{1 - \sqrt{1 - 1/x}}{1 + \sqrt{1 - 1/x}} + i\pi \right) \right], \quad x \ge 1.
\end{aligned} \tag{52}$$

The most important ingredient above is a_V which is an unknown parameter representing the vector meson exchange contributions to the B amplitude. A fit to the decay rate (using $B(K_L \to \pi^0\gamma\gamma) = 1.7 \times 10^{-6}$ [18]) and $\gamma\gamma$ spectrum in $K_L \to \pi^0\gamma\gamma$ indicates a value around $a_V = -0.96$. This parameter was very important in increasing the chiral prediction of the decay rate to be in agreement with experiment. We have explored the sen-

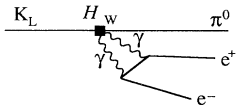

FIG. 9. CP nonviolating diagram involving two photons coupling to e^+e^-. The notation for the vertices is as in Fig. 2.

sitivity of this parameter to changes in the analysis and have found that 25% changes in the dispersive treatment lead to a factor of 2 change in a_V, so that this value is still quite uncertain.

Several authors [14,17,19] have calculated the contribution of the on-shell two-photon intermediate state to $K_L \to \pi^0 e^+ e^-$. Although this is sometimes referred to as the absorption contribution, it is not the full absorption part since there is a further cut due to on-shell pions. Besides this, the full CP-conserving amplitude also receives contributions from the dispersive part of the amplitude, with off-shell photons (and pions). The calculation of this is complicated by the sensitivity of the loop integral to high momentum, as the Feynman diagram of Fig. 9 will diverge if we treat the B amplitude as a constant in q_1^2 and q_2^2. However, the remedy to this is well known; the coupling of virtual photons to hadrons is governed by form factors which lead to suppression of the couplings at high q^2. We will include an estimate of these form factors, and this will allow us to calculate the dispersive component of the CP-conserving amplitude.

The two photon loop integral in the limit $m_e \to 0$ is given by

$$\mathcal{M}(K_L \to \pi^0 e^+ e^-)_{\rm CPC} = \frac{G_8 \alpha}{4\pi m_K^2} \int \frac{d^4 l}{(2\pi)^4} \frac{B(k+k') F(l+k) F(l-k')}{l^2 (l+k)^2 (l-k')^2} \times \{ \not{p}[l^2 + p\cdot(k-k') - p\cdot l\, l\cdot(k-k') + 2p\cdot lk\cdot k' - p\cdot kl\cdot k' - p\cdot k' l\cdot k] + \not{l}[(p\cdot l)^2 + p\cdot lp\cdot(k-k')]\}. \tag{53}$$

Here $F(q^2)$ are the form factors for the virtual photon couplings. The structure above is certainly an approximation, as in general the virtual photon dependence need not be only an overall factor of $F(q^2)$. However, the above form would be sufficient to capture the kinematic variation if only one photon is off-shell [given an appropriate $F(q^2)$]. Since we only need a minor form factor suppression to tame the logarithmic divergencies, we feel that this structure will be sufficient for our estimate. We choose

$$F(q^2) = \frac{-m_V^2}{q^2 - m_V^2}, \tag{54}$$

which is a good representation of almost any mesonic form factor, with $m_V \approx m_\rho$. Neglecting terms which are suppressed by powers of $1/m_\rho^2$, we find the amplitude of Eq. (50) above, with

$$K = \frac{B(x)}{16\pi^2 m_K^2} \left[\frac{2}{3} \ln\left(\frac{m_\rho^2}{-s}\right) - \frac{1}{4} \ln\left(\frac{-s}{m_e^2}\right) + \frac{7}{18} \right], \tag{55}$$

where $s = (k_{e^-} + k_{e^+})^2$. The log factor is of course expected, since the photon "absorptive" part comes from the expansion $\ln(-s) = \ln s + i\pi$.

This representation of the amplitude leads to a CP-conserving branching ratio of

$$B(K_L \to \pi^0 e^+ e^-)_{\rm CPC} = 4.89 \times 10^{-12} \tag{56}$$

for $a_V = -0.96$. More generally we show the CP-conserving branching ratio vs a_V in Fig. 10. Note that while for many values of a_V the CP-conserving rate is small compared to the CP-violating rate of previous sections, these two rates are comparable for some range of parameters. Note that there is no interference in the rate between the CP-conserving and violating components, so that the rates just add, as shown in Fig. 11. However, there can be a CP-odd asymmetry in the electron-positron energies, which we turn to in the next section.

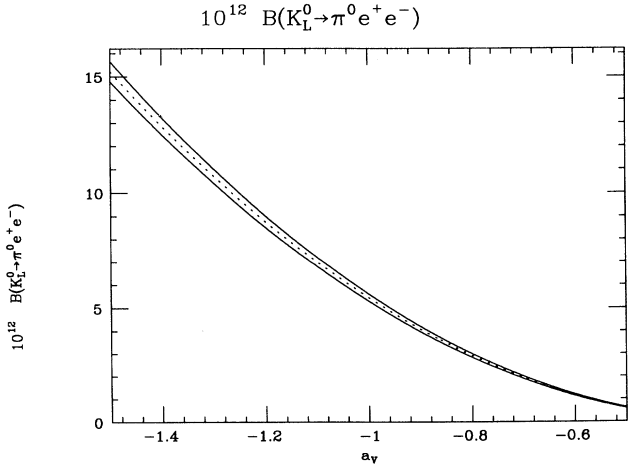

FIG. 10. The CP-conserving branching ratio $B(K_L \to \pi^0 e^+ e^-)_{\rm CPC}$ is plotted against a_V. The convention for the solid and dashed curves is the same as for Fig. 6.

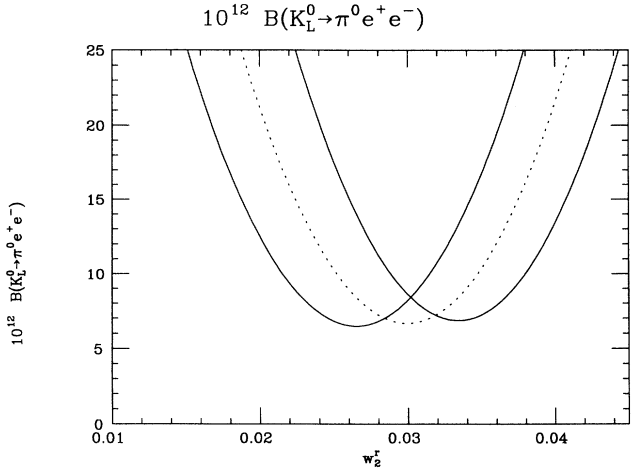

FIG. 11. The complete branching ratio $B(K_L \to \pi^0 e^+ e^-)$ is plotted against w_2. The convention for the solid and dashed curves is the same as for Fig. 6. $a_V = -0.96$ is assumed.

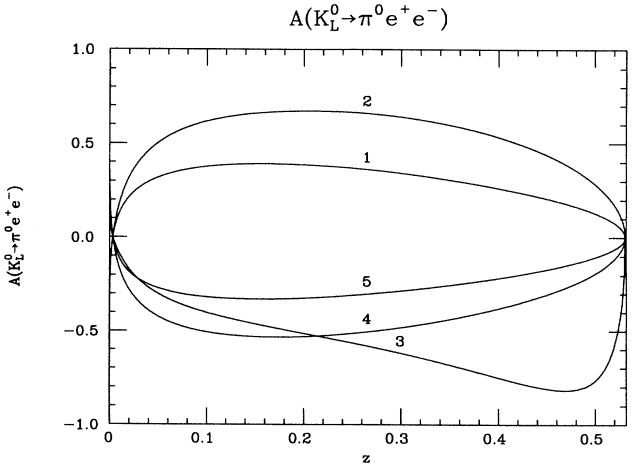

FIG. 12. The differential asymmetry $A(z)$ is plotted against $z \equiv (k_{e^-} + k_{e^+})^2/m_K^2$ for $w_2 = 1 \times 10^{-2}$ (curve 1), 2×10^{-2} (curve 2),..., 5×10^{-2} (curve 5), in the case when there is no direct CP violation. $a_V = -0.96$ is assumed.

VII. THE ELECTRON ENERGY ASYMMETRY

When both CP-violating and CP-conserving amplitudes contribute to the decay, there will be an asymmetry in the electron-positron energy distribution

$$A = \frac{N(E_+ > E_-) - N(E_+ < E_-)}{N(E_+ > E_-) + N(E_+ < E_-)}. \tag{57}$$

This will be quite large if the two amplitudes are comparable. In contrast with the overall decay rate, this asymmetry is an unambiguous signal of CP violation. It may be even more useful if it can be used to prove the existence of direct CP violation. This can occur because the asymmetry is sensitive to the phase of the CP-violating amplitude, and mass-matrix CP violation has a unique phase (that of ϵ), while direct CP violation will in general have a different phase.

For the electron energy asymmetry to be useful as a diagnostic of the form of CP violation, the CP-conserving two photon amplitudes must be well known. As we discussed in the previous section, it is reasonable to expect that this will be true in the future after further phenomenology of $K_L \to \pi^0\gamma\gamma$. For illustrative purposes, we will use $a_V = -0.96$. The analysis below will need to be redone in the future if this value of a_V changes significantly. However, the pattern of the analysis and the general conclusions will be valid for a wide range of values of a_V.

The amplitudes involved have been given in the previous section. Note that the two photon amplitude has both real and imaginary parts, the mass-matrix CP-violating amplitude has a phase of 45°, while the direct component is purely imaginary. The asymmetry is proportional to the imaginary part of B times the real part of d_V minus the product of the real part of B and imaginary part of d_V. The asymmetry may be defined in differential form

$$\frac{d\Gamma}{dz}(E_+ > E_-) = \int_0^{\lambda^{1/2}(1,z,r^2)/2} dy \frac{d\Gamma}{dydz},$$
$$\frac{d\Gamma}{dz}(E_+ < E_-) = \int_{-\lambda^{1/2}(1,z,r^2)/2}^{0} dy \frac{d\Gamma}{dydz},$$
$$\lambda^{1/2}(1,z,r^2) = 1 + z^2 + r^4 - 2z - 2r^2 - 2r^2 z,$$
$$r = \frac{m_\pi}{m_K},$$
$$A(z) = \frac{d\Gamma(E_+ > E_-)/dz - d\Gamma(E_+ < E_-)/dz}{d\Gamma(E_+ > E_-)/dz + d\Gamma(E_+ < E_-)/dz},$$
$$z \equiv (k_{e^-} + k_{e^+})^2/m_K^2. \tag{58}$$

In Fig. 12 we plot the differential asymmetry for several values of w_2 in the case when there is not direct

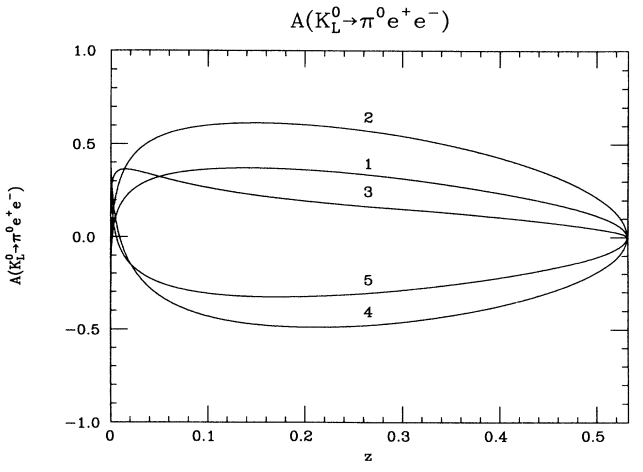

FIG. 13. Same as Fig. 12 for $\mathrm{Im}\lambda_t = 10^{-4}$.

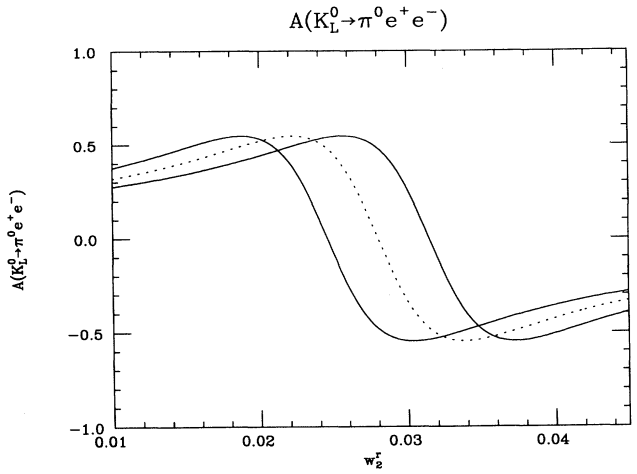

FIG. 14. The integrated asymmetry is plotted vs w_2 in the case when there is no direct CP violation. The convention for the solid and dashed curves is the same as for Fig. 6. $a_V = -0.96$ is assumed.

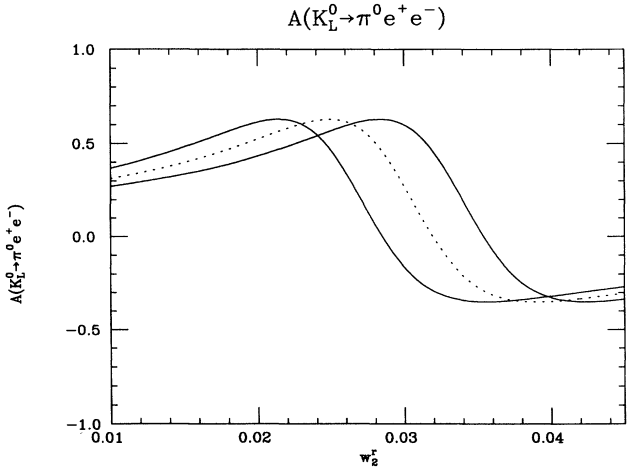

FIG. 15. Same as Fig. 14 for $\mathrm{Im}\lambda_t = 10^{-4}$.

CP violation. Figure 13 gives the same information for $\mathrm{Im}\lambda_t = 10^{-4}$. We see that the asymmetry is sizable for many values of w_2 and that it depends significantly on direct CP violation, even possibly changing sign. The integrated asymmetry is plotted versus w_2 in Figs. 14 and 15.

Both the decay rate and the asymmetry depend on w_S, and this forms the main uncertainty in the analysis. However, it is possible to remove this uncertainty by measuring both observables. For a given value of the CP-conserving amplitude, there is a strict correlation between the two. In Fig. 16 we plot the values of the branching ratio and the integrated asymmetry A as one varies w_2. We see that the curves with and without direct CP violation are well separated for much of the range. To the extent that we understand the CP-conserving amplitude, this can be used as a diagnostic test for direct CP violation.

VIII. TIME-DEPENDENT INTERFERENCE OF $K_1, K_2 \to \pi^0 e^+ e^-$

Littenberg [20] has suggested a time-dependent analysis of a state starting out as a K^0 in order to extract maximal information about the decay mechanism. This is far more demanding experimentally then simply measuring K_L or K_S decays separately. However, we analyze this technique in order to assess its usefulness.

A state that at $t = 0$ is a K^0 will evolve into a mixture of K_L and K_S:

$$|K^0(t)\rangle = \frac{1}{(1+\epsilon)\sqrt{2}}\{e^{-iH_S t}[|K_1\rangle + \epsilon|K_2\rangle] + e^{-iH_L t}[|K_2\rangle + \epsilon|K_1\rangle]\}, \tag{59}$$

where

$$H_j = m_j - i\frac{\Gamma_j}{2}, \quad j = S, L. \tag{60}$$

Ignoring small effects such as second-order CP violation and direct CP-violating components in the parameter ϵ, we then have a time development proportional to

$$|\langle \pi^0 e^+ e^- | \mathcal{H} | K^0(t)\rangle|^2 \approx \frac{1}{2}\Big\{|A_S|^2 e^{-\Gamma_S t} + |\epsilon A_S + A_{\mathrm{dir}} + A_{\mathrm{CPC}}|^2 e^{-\Gamma_L t} + 2\mathrm{Re}[(\epsilon A_S + A_{\mathrm{dir}} + A_{\mathrm{CPC}})A_S^* e^{-i(m_L - m_S)t}]e^{-(\Gamma_L+\Gamma_S)t/2}\Big\}. \tag{61}$$

Here A_{dir}, ϵA_S, and A_{CPC} are the amplitudes analyzed in Secs. III, IV, and VI, respectively. Measurements at early time ($t \ll 1/\Gamma_S$) determine $\Gamma(K_S \to \pi^0 e^+ e^-)$ while at the late time ($t \gg 1/\Gamma_S$) one observes $\Gamma(K_L \to \pi^0 e^+ e^-)$. These contain the information described in preceding sections. However, in the interference region $t = O(1/(m_L - m_S)) = O(1/\tau_S)$, we obtain extra information about the separate contributions to the decay

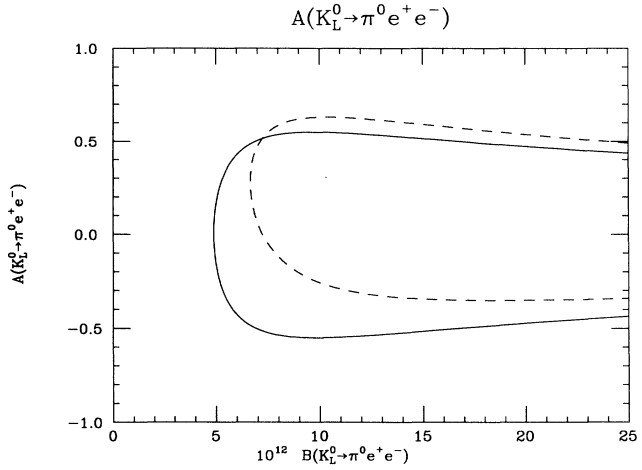

FIG. 16. The integrated asymmetry A is plotted vs the branching ratio $B(K_L \to \pi^0 e^+ e^-)$ as one varies w_2. $a_V = -0.96$ is assumed. The solid curve describes the case when there is no direct CP violation, the dashed curve is for $\mathrm{Im}\lambda_t = 10^{-4}$.

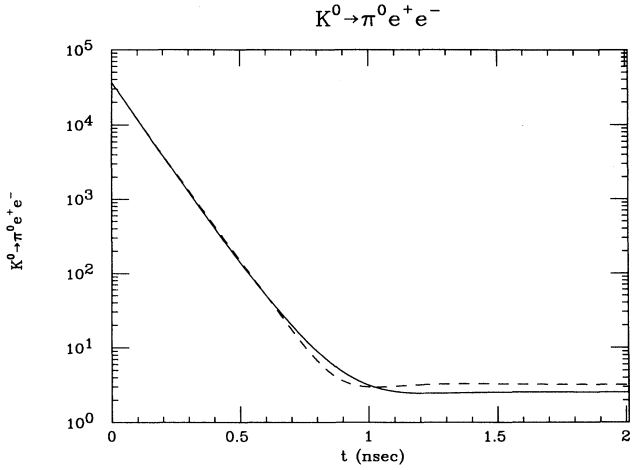

FIG. 17. The normalized time distribution of $K^0 \to \pi^0 e^+ e^-$ decays is plotted vs time t in nsecs. $a_V = -0.96$ is assumed. The solid curves describes the case when there is no direct CP violation, the dashed curve is for $\mathrm{Im}\lambda_t = 10^{-4}$.

amplitude.

In Fig. 17 we show the time-dependent signal for the cases of pure mass-matrix CP violation and the addition of direct CP violation, using the analysis of the previous sections with $w_2 = 4L_9$. We see that the shape of the interference region does differentiate these two cases, but that for the case studied the dependence on direct CP violation is not so large as to allow an easy experimental determination.

IX. SUMMARY

Because there are three possible contributions to $K_L \to \pi^0 e^+ e^-$, the analysis has multiple issues which theory must address. We have provided an updated analysis of all of the components. The goal of identifying direct CP violation will not be easily accomplished. The decay rate by itself suffers from a severe uncertainty in the analysis of the mass-matrix contributions. In the chiral analysis there is a free parameter, w_2, which is not fixed experimentally, and which has a strong influence on the decay rate. Measuring the related rate of $K_S \to \pi^0 e^+ e^-$ would determine this parameter and will likely allow us to determine whether or not direct CP violation is present.

Alternatively if the K_S branching ratio is not measured it may be possible to signal direct CP violation using the asymmetry in the e^+, e^- energies. The direct and mass-matrix CP violations have different phases, and the asymmetry is sensitive to their difference. There exist some combinations of the parameters where there remains some ambiguity, but for sizable portions of the parameter space direct CP violation can be signaled by a simultaneous measurement of the decay rate and the energy asymmetry, as illustrated in Fig. 16.

Progress in the theoretical analysis is possible, especially in the CP-conserving amplitude which proceeds through the two photon intermediate state. Here both a better phenomenological understanding of the related decay $K_L \to \pi^0 \gamma\gamma$, and a better theoretical treatment of the dispersive contribution should be possible in the near future.

ACKNOWLEDGMENTS

We would like to thank B. R. Holstein, J. Kambor, L. S. Littenberg, and G. Valencia for helpful discussions.

[1] L. Wolfenstein, Phys. Rev. Lett. **13**, 562 (1964).
[2] G. Ecker, A. Pich, and E. de Rafael, Nucl. Phys. **B291**, 692 (1987).
[3] G. Ecker, A. Pich, and E. de Rafael, Nucl. Phys. **B303**, 665 (1988).
[4] A. J. Buras, M. E. Lautenbacher, M. Misiak, and M. Münz, Nucl. Phys. **B423**, 349 (1994).
[5] L. Wolfenstein, Phys. Rev. Lett. **51**, 1945 (1983).
[6] S. L. Stone, in *CP Violation and the Limit of the Standard Model, TASI 94*, edited by John F. Donoghue (World Scientific, Singapore, 1995).
[7] G. Altarelli, N. Cabibbo, G. Corbo, L. Maiani, and G. Martinelli, Nucl. Phys. **B207**, 365 (1982).
[8] C. Ramirez, J. F. Donoghue, and G. Burdman, Phys. Rev. D **41**, 1496 (1990).
[9] N. Isgur, D. Scora, B. Grinstein, and M. B. Wise, Phys. Rev. D **39**, 799 (1989).
[10] M. Wirbel, B. Stech, and U. Bauer, Z. Phys. C **29**, 637

(1985).
[11] J. Körner and G. A. Schuler, Z. Phys. C **37**, 511 (1988).
[12] J. Kambor, J. Missimer, and D. Wyler, Nucl. Phys. **B346**, 17 (1990).
[13] J. Kambor, J. Missimer, and D. Wyler, Phys. Lett. B **261**, 496 (1991).
[14] G. Ecker, A. Pich, and E. de Rafael, Phys. Lett. B **237**, 481 (1990).
[15] J. F. Donoghue, E. Golowich, and B. R. Holstein, Phys. Rev. D **30**, 587 (1984).
[16] L. S. Littenberg and G. Valencia, Annu. Rev. Nucl. Part. Sci. **43**, 729 (1993).
[17] A. G. Cohen, G. Ecker, and A. Pich, Phys. Lett. B **304**, 347 (1993).
[18] G. D. Barr *et al.*, Phys. Lett. B **242**, 523 (1990); **284**, 440 (1992).
[19] G. Ecker, A. Pich, and E. de Rafael, Phys. Lett. B **189**, 363 (1987); L. Cappiello and G. D'Ambrosio, Nuovo Cimento A **99**, 155 (1988); L. M. Sehgal, Phys. Rev. D **38**, 808 (1988); J. Flynn and L. Randall, Phys. Lett. B **216**, 221 (1989); P. Ko and J. Rosner, Phys. Rev. D **40**, 3775 (1989); P. Ko, *ibid.* **41**, 1531 (1990); J. Bijnens, S. Dawson, and G. Valencia, *ibid.* **44**, 3555 (1991); T. Hambye, Int. J. Mod. Phys. A **7**, 135 (1992); L. Cappiello, G. D'Ambrosio, and M. Miragliuolo, Phys. Lett. B **298**, 423 (1993); P. Heiliger and L. M. Sehgal, Phys. Rev. D **47**, 4920 (1993); J. Kambor and B. R. Holstein, *ibid.* **49**, 2346 (1994).
[20] L. S. Littenberg, Report No. BNL-42892, 1989 (unpublished); Vancouver CP Workshop '88, p. 19.